the FEBS Journal

Factor VIIIa regulates substrate delivery to the intrinsic factor X-activating complex

Mikhail A. Panteleev[1,2], Natalya M. Ananyeva[1,*], Nicholas J. Greco[1,†], Fazoil I. Ataullakhanov[2,3,4] and Evgueni L. Saenko[1,*]

1 Jerome H. Holland Laboratory for the Biomedical Sciences, American Red Cross, Rockville, Maryland, USA
2 Laboratory of Physical Biochemistry of Blood, National Research Center for Hematology, Russian Academy of Medical Sciences, Moscow, Russia
3 Laboratory of Metabolic Modeling and Bioinformatics, Institute of Theoretical and Experimental Biophysics, Moscow, Russia
4 Faculty of Physics, Moscow State University, Russia

Keywords
blood coagulation; factor VIIIa; factor IXa; factor X; flow cytometry

Correspondence
M.A. Panteleev, Laboratory of Physical Biochemistry of Blood, National Research Center for Hematology, Russian Academy of Medical Sciences, Novozykovskii pr. 4a, Moscow, 125167, Russia
Fax: +7 095 212 8870
Tel: +7 095 212 3522
E-mail: mapanteleev@yandex.ru
Website: http://physbio.hc.comcor.ru

***Present address**
Department of Biochemistry & Molecular Biology, University of Maryland School of Medicine, Baltimore, USA

†Present address
Department of Medicine, Case Western Reserve University School of Medicine, Cleveland, OH, USA

Portions of this work were presented at the 30th FEBS Congress–9th IUBMB Conference (Budapest, Hungary, 2–7 July 2005) and published in abstract form in *FEBS Journal*, 2005, **272** (Suppl. 1), 405.
Mikhail A. Panteleev and Natalya M. Ananyeva contributed equally to this work.

(Received 8 August 2005, revised 19 October 2005, accepted 22 November 2005)

doi:10.1111/j.1742-4658.2005.05070.x

Activation of coagulation factor X (fX) by activated factors IX (fIXa) and VIII (fVIIIa) requires the assembly of the enzyme–cofactor–substrate fIXa–fVIIIa–fX complex on negatively charged phospholipid membranes. Using flow cytometry, we explored formation of the intermediate membrane-bound binary complexes of fIXa, fVIIIa, and fX. Studies of the coordinate binding of coagulation factors to 0.8-μm phospholipid vesicles (25/75 phosphatidylserine/phosphatidylcholine) showed that fVIII (fVIIIa), fIXa, and fX bind to 32 700 ± 5000 (33 200 ± 14 100), 20 000 ± 4500, and 30 500 ± 1300 binding sites per vesicle with apparent K_d values of 76 ± 23 (71 ± 5), 1510 ± 430, and 223 ± 79 nM, respectively. FVIII at 10 nM induced the appearance of additional high-affinity sites for fIXa (1810 ± 370, 20 ± 5 nM) and fX (12 630 ± 690, 14 ± 4 nM), whereas fX at 100 nM induced high-affinity sites for fIXa (541 ± 67, 23 ± 5 nM). The effects of fVIII and fVIIIa on the binding of fIXa or fX were similar. The apparent Michaelis constant of the fX activation by fIXa was a linear function of the fVIIIa concentration with a slope of 1.00 ± 0.12 and an intrinsic K_m value of 8.0 ± 1.5 nM, in agreement with the hypothesis that the reaction rate is limited by the fVIIIa–fX complex formation. In addition, direct correlation was observed between the fX activation rate and formation of the fVIIIa–fX complex. Titration of fX, fVIIIa, phospholipid concentration and phosphatidylserine content suggested that at high fVIIIa concentration the reaction rate is regulated by the concentration of free fX rather than of membrane-bound fX. The obtained results reveal formation of high-affinity fVIIIa–fX complexes on phospholipid membranes and suggest their role in regulating fX activation by anchoring and delivering fX to the enzymatic complex.

Abbreviations
BSA, bovine serum albumin; DiIC16(3), 1,1′-dihexadecyl-3,3,3′,3′-tetramethylindocarbocyanine perchlorate; fVIII(a), (activated) factor VIII; fIX(a), (activated) factor IX; fIXa-EGR, active-site-inhibited Glu-Gly-Arg-fIXa; fX(a), activated factor X; PtdCho, phosphatidylcholine; PPACK, Phe-Pro-Arg-chloromethyl ketone; PtdSer, phosphatidylserine; S-2765, *N*-α-((benzyloxy)carbonyl)-D-Arg-Gly-Arg-*p*-nitroanalide dihydrochloride.

The intrinsic factor X (fX)-activating complex is composed of the enzyme (factor IXa; fIXa), the substrate (fX), and the cofactor (factor VIIIa; fVIIIa) assembled on a negatively charged phospholipid surface [1,2]. FIXa is a two-chain vitamin K-dependent serine protease which activates fX by cleaving a single Arg194–Ile195 peptide bond in the fX molecule [3]. Heterotrimeric (A1/A2/A3–C1–C2) fVIIIa [4] is a cofactor that amplifies the rate of this reaction by several orders of magnitude [1,5]. The exact mechanisms of the fX-activating complex assembly and of the fVIIIa cofactor action in the intrinsic tenase remain insufficiently understood [2].

Numerous studies have reported rates [6–8], equilibrium-binding parameters [9–11], and mechanisms [12,13] for the individual binding of fIXa, fVIIIa, and fX to phospholipid membranes. Interaction of fIXa and fVIIIa within the fX-activating complex and formation of the fIXa–fVIIIa complex have been also investigated by several groups [5,14–16], which identified interaction sites, association parameters, and contributions of different fVIIIa domains in the stimulation of the fIXa activity. However, formation and function of the fIXa–fX and fVIIIa–fX complexes is less studied. The fVIIIa–fX binding has been investigated in a solid-phase binding assay [17]; interaction with the affinity of 1–3 μM was observed between the serine protease domain of fX and COOH-terminal region of the A1 domain of fVIIIa [17,18]. However, the interaction of fVIIIa and fX on phospholipid membranes and its role in activation of fX have not been studied. It remains unclear whether this interaction is essential for the activation of fX [2] or for the formation of the intermediate fVIII(a)–fX complex in the course of assembly of the fX-activating complex [19,20] or, probably, for the fVIII activation by fXa [21].

Previously, we approached the problem of the assembly of the fX-activating complex using mathematical modeling [19]. We hypothesized that the fX-activating complex is assembled via formation of two intermediate binary complexes, fIXa–fVIIIa and fVIIIa–fX. The goal of this study was to experimentally explore the roles of the binary complexes formed by fIXa, fVIIIa, and fX in the assembly and functioning of the fX-activating complex. We have shown that all three possible binary complexes, i.e. fIXa–fVIIIa, fIXa–fX, and fVIIIa–fX, are formed in the course of fX activation, formation of fIXa–fVIIIa and fVIIIa–fX being most significant. We obtained experimental evidence that formation of the cofactor–substrate fVIIIa–fX complex regulates the rate of fX activation. This study suggests an additional function for fVIIIa in providing high-affinity binding sites for fX on the membrane surface and in delivering the substrate to the fX-activating complex.

Results

Equilibrium coordinate binding of fVIII, fIXa, and fX to phospholipid vesicles

To explore interaction between components of the fX-activating complex on a phospholipid membrane, we studied the binding of fluorescein-labeled fVIII, fVIIIa, fIXa–EGR, and fX in various combinations with each other to synthetic PtdSer/PtdCho (25/75) vesicles using flow cytometry. The representative binding curves are shown in Fig. 1 and the mean binding parameters calculated from three independent experiments are summarized in Table 1. The binding curves for individual factors were fitted with a standard one-site binding model (rectangular hyperbola equation) [19]. FVIII bound to 32 700 ± 5000 binding sites per vesicle with an apparent K_d of 76 ± 23 nM and activated cofactor demonstrated similar binding parameters. Under the conditions used in this study, the molar concentration of binding sites (estimated as 50–100 nM at 5 μM of phospholipid on the basis of reported binding stoichiometries) [10,12] could significantly exceed ligand concentration. Therefore, the obtained K_d values represent apparent constants, which are equal to the sum of true K_d values and molar concentrations of binding sites for the respective factor. Thus, apparent K_d of 76 nM, determined for fVIII, corresponds to true K_d (in the range of 5–10 nM) reported earlier [8,10]. The apparent affinities of fVIII and fVIIIa are similar because the method does not allow observation of the difference in true affinities for fVIIIa and fVIII reported by us earlier [8].

In agreement with previous reports [13], fVIII binding to the phospholipid membrane was not apparently affected by fIXa–EGR and fX, present either individually or in combination (Fig. 1A, Table 1). In contrast, fIXa–EGR binding at low concentrations was increased by both fVIII and fX (Fig. 1B), though maximal binding was decreased. The binding curves for fIXa–EGR in the presence of fVIII or/and fX could not be fitted using a one-site binding model. The additional criteria were nonlinearity of the fitting curves in double-reciprocal plots and a decrease in chi-square value upon transition from the one-site model to the two-site model (data not shown). The fVIII- and fX-dependent binding of fIXa–EGR was quantitated by subtracting fIXa–EGR binding in the absence of fVIII or fX from the total fIXa–EGR binding as

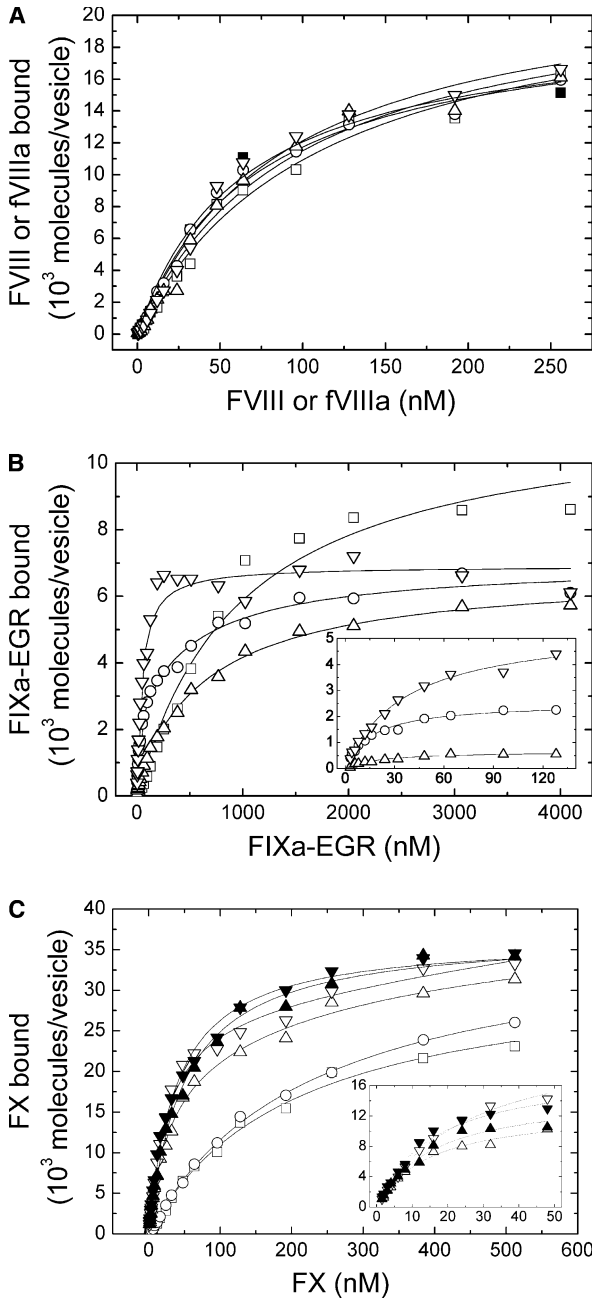

Fig. 1. Cooperative binding of the components of intrinsic tenase to phospholipid vesicles. Coagulation factors at indicated concentrations were incubated with phospholipid vesicles (5 μM) and with other factors at fixed concentrations at 37 °C for 15 min, and the binding was determined by flow cytometry as described in Experimental Procedures. (A) Binding of fVIII either alone (□) or in the presence of 10 nM fIXa–EGR (○), 100 nM fX (△), both fIXa–EGR and fX (▽), or activated by 1 nM of thrombin (■). (B) Binding of fIXa–EGR: either alone (□) or in the presence of 10 nM fVIII (○), 100 nM fX (△), or both fVIII and fX (▽). (C) Binding of fX: either alone (□) or in the presence of 10 nM fIXa-EGR (○), 10 nM fVIII (△), both fIXa–EGR and fVIII (▽), 10 nM fVIIIa (▲), or both fIXa–EGR and fVIIIa (▼). The insets show the specific binding of fIXa–EGR (B) and fX (C) in the presence of other factors, obtained by subtraction of the fIXa-EGR or fX binding alone from the total binding. Solid lines show nonlinear least-squares fit of the experimental data to the rectangular hyperbola equation.

described in Experimental Procedures (see inset in Fig. 1B) and was fitted with a one-site model. We found that fVIII and fX induced the appearance of additional 1810 ± 370 and 541 ± 67 high-affinity sites for fIXa, respectively, and a combination of fVIII and fX induced the appearance of 4410 ± 580 sites (Table 1). The binding of fX was not affected by fIXa–EGR, whereas fVIII and fVIIIa enhanced it dramatically, increasing both the apparent affinity and the maximal binding (Fig. 1C). Subtraction analysis demonstrated that fVIII (fVIIIa) at 10 nM induced the appearance of additional 12 630 ± 690 (11 700 ± 3300) high-affinity binding sites for fX, with a K_d value of 14 ± 4 nM (16.0 ± 0.4 nM).

To further characterize the interaction between the factors on a phospholipid surface, we carried out parallel titrations of fVIII, fVIIIa, fIXa–EGR, and fX. In Fig. 2, the binding of increasing concentrations of fIXa–EGR and fX is plotted as a function of the binding of fVIII (Fig. 2A, D), fVIIIa (Fig. 2B) and fX (Fig. 2C) to vesicles. The concentrations of bound factors were determined in parallel experiments, based on the conclusion of the previous experiment (Fig. 1) that the binding of fVIII(a) is unaffected by fIXa–EGR and fX, and the binding of fX is unaffected by fIXa. A dose-dependent increase in the binding of fIXa–EGR and fX accompanying an increase in the bound fVIII (Fig. 2A and D, respectively) and fVIIIa (Fig. 2B) levels indicated formation of the fIXa–fVIII(a) and fX–fVIII(a) complexes on the phospholipid membrane. A positive effect of fX on fIXa–EGR binding was also observed at low concentrations of fIXa–EGR and fX (Fig. 2C). At higher concentrations, there was inhibition suggesting a competitive displacement of fIXa–EGR from the phospholipid surface by fX. Thus, the equilibrium binding studies revealed the formation of fIXa–fVIII and fX–fVIII binary complexes on the phospholipid surface.

Effect of fVIII on the kinetics of the fX binding to phospholipid vesicles

The intriguing result of the equilibrium binding experiments that fVIII and fVIIIa bind fX with the affinity as high as that of the fVIII(fVIIIa)–fIXa interaction suggests that the fVIII(a)–fX complex is actively formed during the assembly of intrinsic tenase. To test

Table 1. Parameters for the binding of intrinsic tenase components to phospholipid vesicles. Binding parameters shown are the means (± SE) for three separate experiments. Phospholipid concentration was 5 μM. Other experimental conditions are described in the legend to Fig. 1.

Binding ligand	Fixed component(s)	N_{max} (molecules/vesicle)	K_d (nM)
fVIII (0–256 nM)	None	32 700 ± 5000	76 ± 23
	fIXa–EGR (10 nM)	39 700 ± 11 000	77 ± 8
	fX (100 nM)	39 800 ± 8800	73 ± 16
	fIXa (10 nM), fX (100 nM)	41 600 ± 9800	68 ± 14
fVIIIa (0–256 nM)	None	33 200 ± 14 100	71 ± 5
fIXa–EGR (0–4096 nM)	None	20 000 ± 4500	1500 ± 430
	fVIII (10 nM)[a]	1810 ± 370	20 ± 5
	fX (100 nM)[a]	541 ± 67	23 ± 5
	fVIII (10 nM), fX (100 nM)[a]	4410 ± 580	48 ± 10
fX (0–512 nM)	None	30 500 ± 1300	223 ± 79
	fIXa-EGR (10 nM)	34 500 ± 2900	203 ± 73
	fVIII (10 nM)[a]	12 630 ± 690	14 ± 4
	fIXa (10 nM), fVIII (10 nM)[a]	22 040 ± 800	22 ± 7
	fVIIIa (10 nM)[a]	11 700 ± 3300	16.0 ± 0.4
	fIXa (10 nM), fVIIIa (10 nM)[a]	21 000 ± 2900	32 ± 17

[a] These parameters describe specific binding and were determined from the curves (see insets in Fig. 1B,C) obtained by subtraction of the nonspecific binding from the total binding.

whether formation of this complex is kinetically efficient, the fX association with phospholipid vesicles was studied at increasing fX concentrations in the absence or presence of 20 nM fVIII (Fig. 3). A nonlinear least square fit of the experimental data to a decaying exponential model (the reaction following a pseudo-first-order kinetics) yielded kinetic association and dissociation parameters of $k_a = 0.017 \pm 0.007$ nM^{-1}·min^{-1} and $k_{Da} = 1.50 \pm 0.22$ min^{-1} for fX alone ($n = 3$). These values are close to those reported in a recent surface plasmon resonance study of fX binding to synthetic phospholipids membranes [6], although an earlier stopped-flow light scattering study reported two-orders of magnitude greater values for fXa [7]. In the presence of fVIII, these parameters were changed to $k_a = 0.026 \pm 0.012$ nM^{-1}·min^{-1} and $k_{Da} = 0.55 \pm 0.04$ min^{-1} ($n = 3$) indicating a 1.5-fold increase of the association rate and a threefold decrease of the dissociation rate. The average ratios of these constants give the K_d value of 118 ± 33 nM in the absence and 32 ± 14 nM in the presence of fVIII and agree with the values obtained from the equilibrium binding studies (Table 1). Thus, kinetic binding studies showed that formation of the fVIII–fX complex is rapid. Several studies have reported that substrate delivery to the membrane can be a rate-limiting factor in reactions catalyzed by intrinsic tenase and prothrombinase [22,23]. Therefore, the increase in fX affinity was considered an indicator of an important role of fVIIIa in the delivery of the substrate fX to the phospholipid surface.

Role of the fVIIIa–fX complex in activation of fX by intrinsic tenase

We next addressed the role of the binary fVIII(a)–fX complex in activation of fX. Figure 4 shows the fX activation at different fX and phospholipid concentrations. In agreement with previous reports [8], the rate of fX activation initially increased with the increase of the phospholipid concentration, and then decreased, reaching the maximal values at phospholipid concentrations in the range of 10–100 μM (Fig. 4A). The V_{max} of the reaction increased linearly at low lipid concentrations, and reached a plateau at 100 μM phospholipid (Fig. 4B). The K_M value linearly increased within the range of 0.5–1000 μM (Fig. 4C). For subsequent experiments, a phospholipid concentration of 10 μM was chosen, assuming that at this point V_{max} is close to its maximal value (the binding of factors is close to optimal), while inhibitory effects of excess phospholipid surface are not yet observed. We also took into consideration that the procoagulant activity of activated platelets at physiological concentration is equivalent to that of synthetic phospholipid vesicles at micromolar concentrations [24].

To determine whether formation of the fVIIIa–fX complex has an effect on activation of fX, we carried out parallel studies of fX activation and specific (i.e. fVIIIa-dependent) fX binding under identical conditions (Fig. 5A,B) titrating fVIIIa and fX concentrations. Figure 5A shows the rate of fX activation as a function of fVIIIa concentration. In Fig. 5B, this rate

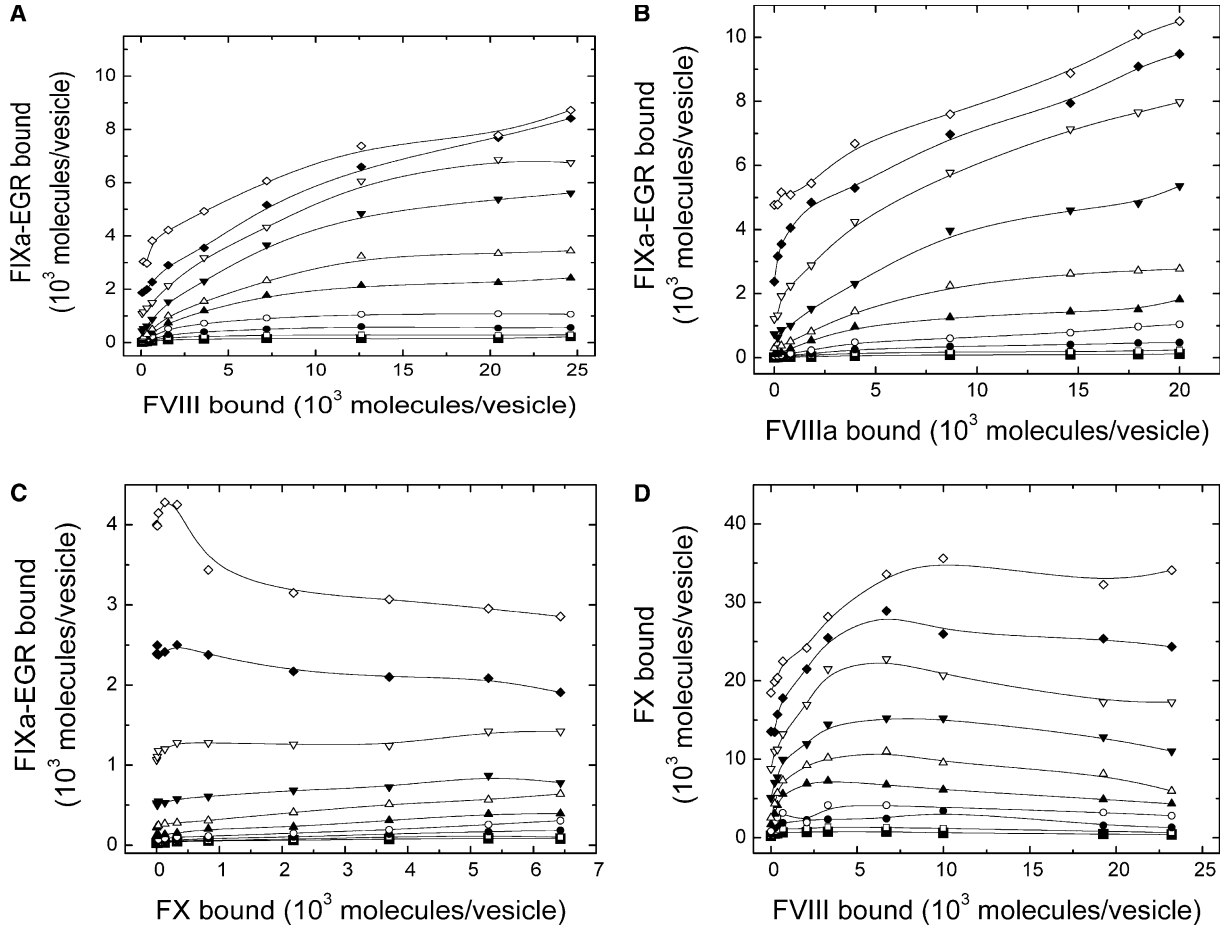

Fig. 2. Interaction of components of intrinsic tenase on phospholipid membrane. FIXa–EGR (A–C) and fX (D) at a concentration of 1 (■), 2 (□), 4 (●), 8 (○), 16 (▲), 32 (△), 64 (▼), 128 (▽), 256 (◆), or 512 (◇) nM were incubated with phospholipid vesicles (5 μM) at 37 °C for 15 min in the presence of increasing concentrations of fVIII (A, D), fVIIIa (B), or fX (C), and the binding was determined as described in Experimental Procedures. The binding of unlabeled factors was estimated in parallel binding experiments with labeled factors. (A) Binding of fIXa–EGR as a function of bound fVIII, added at a concentration from 0 to 256 nM (B) Binding of fIXa–EGR as a function of bound fVIIIa, added at a concentration from 0 to 256 nM (C) Binding of fIXa–EGR as a function of bound fX, added at a concentration from 0 to 256 nM (D) Binding of fX as a function of bound fVIII, added at a concentration from 0 to 256 nM. Solid lines were drawn by B-spline interpolation.

is plotted as a function of fVIIIa-dependent binding of fX (obtained by subtracting the fX binding in the absence of fVIIIa from that in the presence of fVIIIa as described in Experimental Procedures), revealing a correlation between the two parameters. It is noteworthy that fVIIIa in these experiments was in excess over fIXa (0.1 nM) and high above the reported true K_d of 0.07 nM for this interaction [14]. Therefore, these results cannot be explained by a mere increase in the concentration of the fIXa–fVIIIa complex, because fIXa was saturated by fVIIIa within the range of the fVIIIa concentrations used. Thus, the revealed correlation between the rate of fX activation and the level of fVIIIa-dependent binding of fX suggests that formation of the fVIIIa–fX complex is important for the fX activation.

Linear dependence was obtained for K_M of the reaction as a function of fVIIIa (Fig. 5C) with the slope of 1.00 ± 0.12 nM of K_M per 1 nM of fVIIIa and with the intrinsic K_M value (the intersection of the line with the ordinate axis) of 8.0 ± 1.5 nM. Because of saturation of fIXa with fVIIIa, existence of a K_M dependence on fVIIIa cannot be explained unless we assume that the fVIIIa–fX complex is the true substrate in the fX activation. Existence of this dependence does fit well with the assumption that formation of the cofactor–substrate fVIIIa–fX complex on membrane is required for activation of fX by intrinsic tenase. Indeed, regulation of fX activation by its binding to fVIIIa means that K_M of the reaction is equivalent to the K_d of complex formation. The stoichiometry of 1 : 1 would result in the following equation:

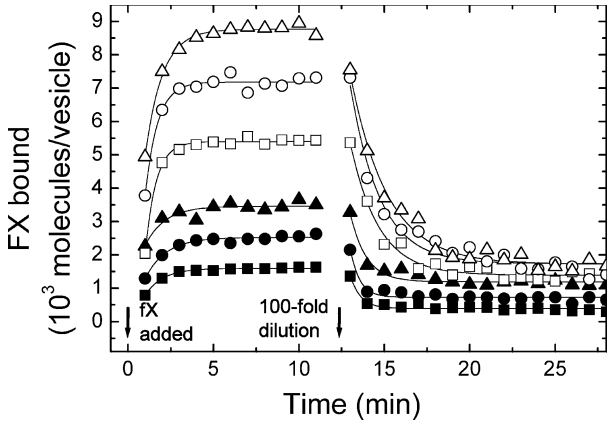

Fig. 3. Effect of fVIII on the kinetics of fX binding to phospholipid vesicles. Factor X at a concentration of 32 (■, □), 64 (●, ○), or 128 (▲, △) nM was incubated with phospholipid vesicles (5 μM) at 37 °C in the absence (filled symbols) or in the presence (open symbols) of fVIII (20 nM). After addition of fX, aliquots were taken and analyzed in a flow cytometer with 1 min intervals. When saturation of the binding was achieved, the sample was rapidly diluted 100-fold, and fX dissociation was monitored. Solid lines represent nonlinear least squares fit of the data to the decaying exponential model to obtain association and dissociation rates.

$$K_d(\text{apparent}) = K_d(\text{intrinsic}) + [\text{fVIIIa}]$$

This should yield a slope of ~1, and an intrinsic K_d of ~8nM is in agreement with this equation and with the apparent affinity of fVIIIa–fX interaction observed in the binding studies (Table 1). Figure 5D displays the rate of fX activation as a function of phospholipid concentration at different fVIIIa concentrations. The stimulating effect of phospholipids becomes saturated at a concentration determined by fVIIIa concentration. The fitting of these curves with the rectangular hyperbola model shows that the half-maximal phospholipid concentration is a linear function of fVIIIa (data not shown), which is also consistent with the model of the rate regulation by the membrane-bound fVIIIa–fX complex.

Studies of the mechanism of substrate delivery

The most probable role of the fVIIIa–fX complex is that fVIIIa binds fX and delivers the substrate to the

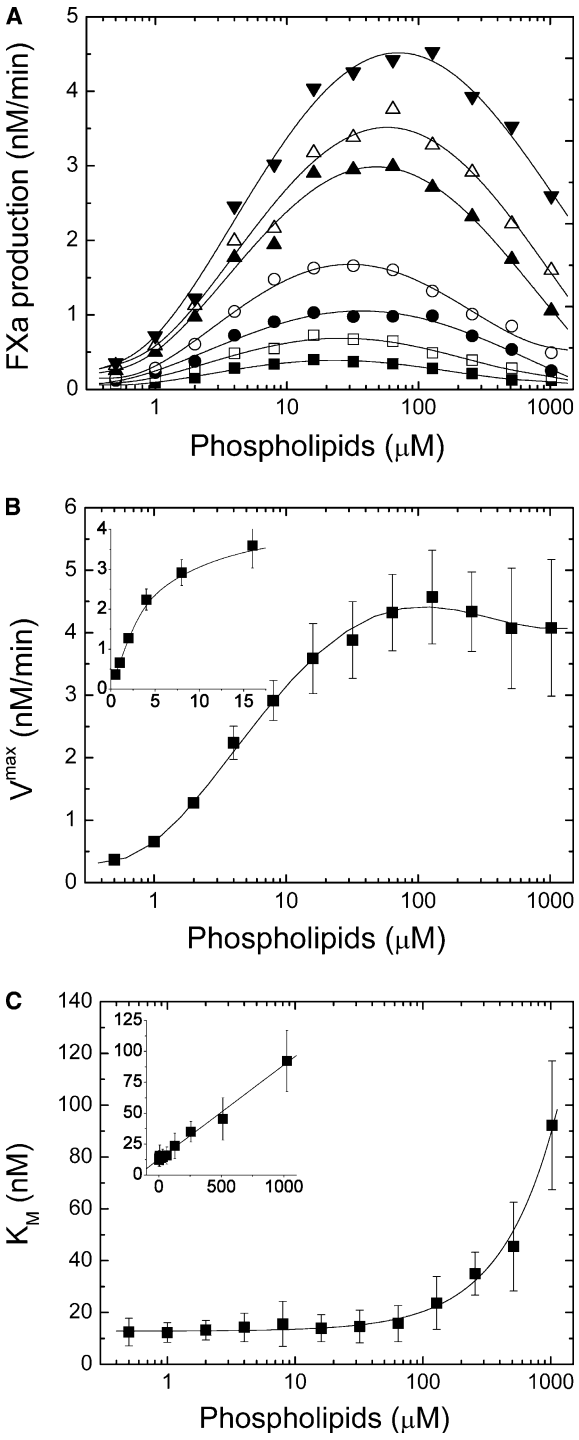

Fig. 4. Kinetics of fX activation by intrinsic tenase complex in the presence of phospholipid vesicles. (A) Initial rate of fX activation by fIXa (30 pM) in the presence of fVIIIa (10 nM) is plotted as a function of phospholipid vesicle concentration. FX concentration was 1.5 (■), 3 (□), 5 (●), 10 (○), 30 (▲), 50 (△), or 100 (▼) nM. Solid lines were drawn using a fourth-order polynomial approximation of the experimental data. (B) Maximal rate of fX activation by intrinsic tenase as a function of phospholipid concentration. Solid line was drawn using a fourth-order polynomial approximation. (C) Michaelis–Menten constant of fX activation by intrinsic tenase as a function of phospholipid concentration. Conditions in (B and C) are the same as in (A). Mean values (± SE) are presented for three experiments. Solid line was drawn using a linear least squares fit. The insets show the results in linear scale.

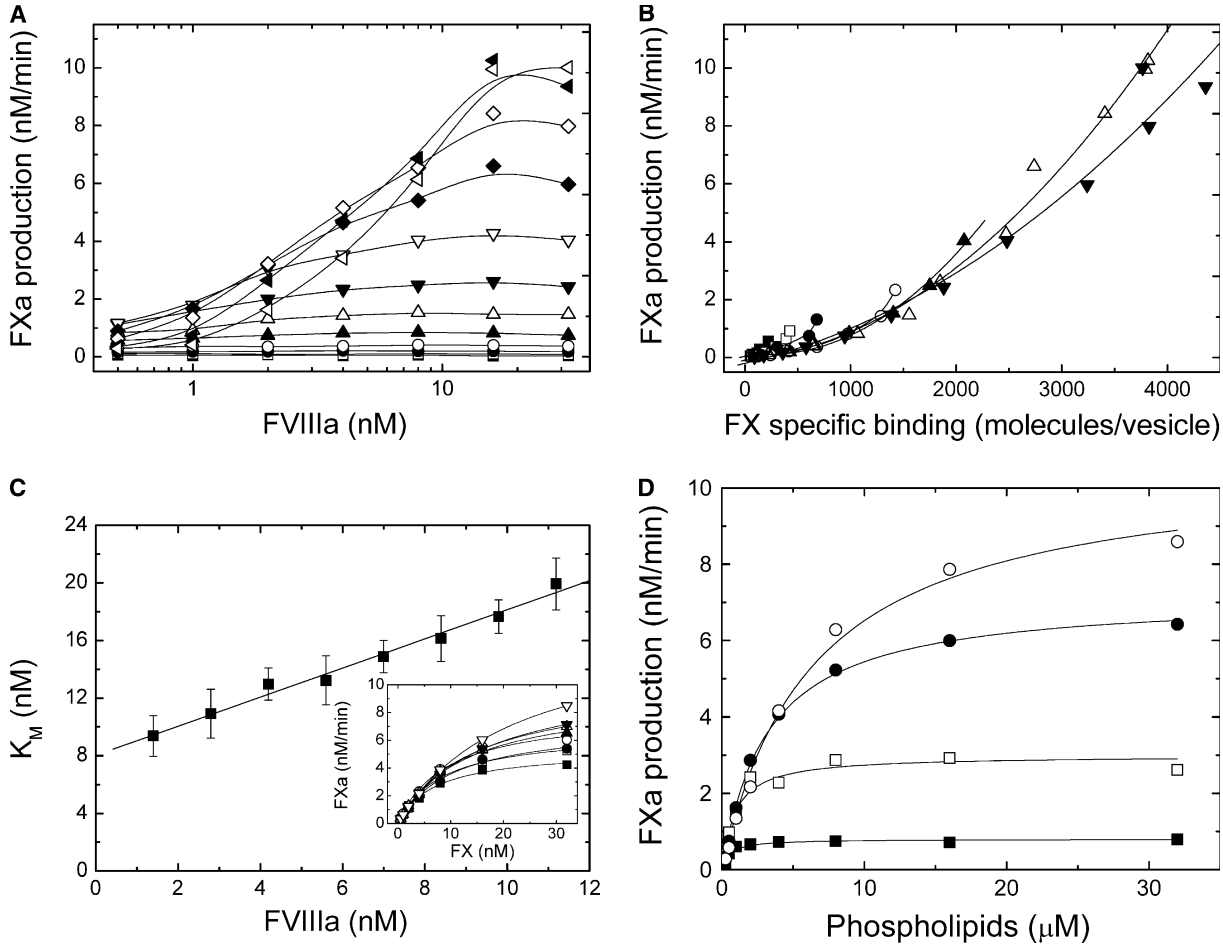

Fig. 5. Correlation between the fVIIIa–fX complex formation and the rate of fX activation. (A) Kinetics of fX activation by fIXa (100 pM) in the presence of fVIIIa at indicated concentrations and phospholipid vesicles (0.8 μm, 10 μm). FX was at 0.125 (■), 0.25 (□), 0.5 (●), 1 (○), 2 (▲), 4 (△), 8 (▼), 16 (▽), 32 (◆), 64 (◇), 128 (◀), or 256 (◁) nM. Solid lines were drawn by B-spline interpolation. (B) FX activation rate shown in panel A is plotted vs. concentration of specifically bound fX. The fVIIIa-dependent binding of fX was determined in parallel experiments by subtracting fVIIIa-independent binding from the total fX binding. FVIIIa was at 0.5 (■), 1 (□), 2 (●), 4 (○), 8 (▲), 16 (△), or 32 (▼) nM. Solid lines were drawn using a second-order polynomial approximation. (C) The Michaelis–Menten constant for fX activation by intrinsic tenase (30 pM fIXa; 10 μM phospholipid vesicles) is plotted as a function of fVIIIa concentration. Mean values (± SE) are presented for four experiments. The inset shows a typical experiment of fX activation at different fVIII concentrations. (D) Kinetics of fX (100 nM) activation by fIXa (30 pM) in the presence of phospholipids at indicated concentrations and fVIIIa at 1.5 (■), 3.5 (□), 10 (●), 20 (○) nM. Solid lines show nonlinear least-squares fit of the experimental data to the rectangular hyperbola equation.

fX-activating complex. There are two possibilities: (a) fX can initially bind to the membrane and subsequently form a complex with fVIIIa by means of two-dimensional diffusion on the membrane (bound substrate model); (b) alternatively, fX can directly bind to membrane-bound fVIIIa from the solution (free substrate model). To distinguish between the two models, an approach proposed earlier by van Rijn *et al.* for prothrombinase was used [25]. FX activation was studied at different phospholipid concentrations (10–1000 μM) and at increasing phosphatidylserine (PtdSer) content (12.5–50%) of vesicles. An excess of phospholipid was used to vary the volume concentration and the membrane density of the substrate fX. The method assumes that the predominant pathway of the substrate delivery (bound or free substrate model) does not change with the increase of phospholipid concentration. A maximal PtdSer content of 50% was chosen to avoid vesicle aggregation occurring at higher PtdSer content in the presence of calcium. In order to study the effect of fVIIIa on the delivery mechanism, the experiments were performed at two fVIIIa concentrations (1.5 and 12 nM); the first concentration is far below the apparent affinity of fVIIIa and fX, whereas

the second is high enough to provide a significant number of high-affinity fVIIIa-dependent fX-binding sites without occupying all sites on phospholipid membrane. The determined kinetic parameters of fX activation were plotted vs. phospholipid concentration (Fig. 6). Analysis of the study [25] gives the apparent value of K_M:

$$K_M(\text{apparent}) = [fX^{free}] + \frac{q[\text{PtdChoPtdSer}]}{K_d^X[fX^{free}]^{-1} + 1} \quad (1)$$

where $[fX^{free}]$ is the concentration of free fX achieved when $[fX^{total}]$ equals K_M, q is the maximal amount of fX that can bind to phospholipid (mol/mol), [PtdChoPtdSer] is the concentration of phospholipids, and K_d^X is the dissociation constant of fX and phospholipid. In both models, apparent K_M is a linear function of [PtdChoPtd Ser]: (a) in the free substrate model, K_M is achieved at the same $[fX^{free}]$ for all concentrations and compositions of phospholipids; (b) in the bound-substrate model, K_M is achieved at the same surface density of fX, i.e. at the same $\frac{q}{K_d^X[fX^{free}]^{-1}+1}$ [25]. However, these models behave differently, when q and K_d^X are varied because of the variation in PtdSer content. The line slope equals to the fX surface density achieved at $[fX] = K_M$. In the bound substrate model, this density is constant at any PtdSer content. In contrast, in the free substrate model, $[fX^{free}]$ is constant. Therefore, the line slope, which equals $\frac{q}{K_d^X[fX^{free}]^{-1}+1}$, will be higher for phospholipid vesicles with more favorable binding parameters (high q and low K_d^X, i.e. high PtdSer content). Further, in the free substrate model, intrinsic K_M

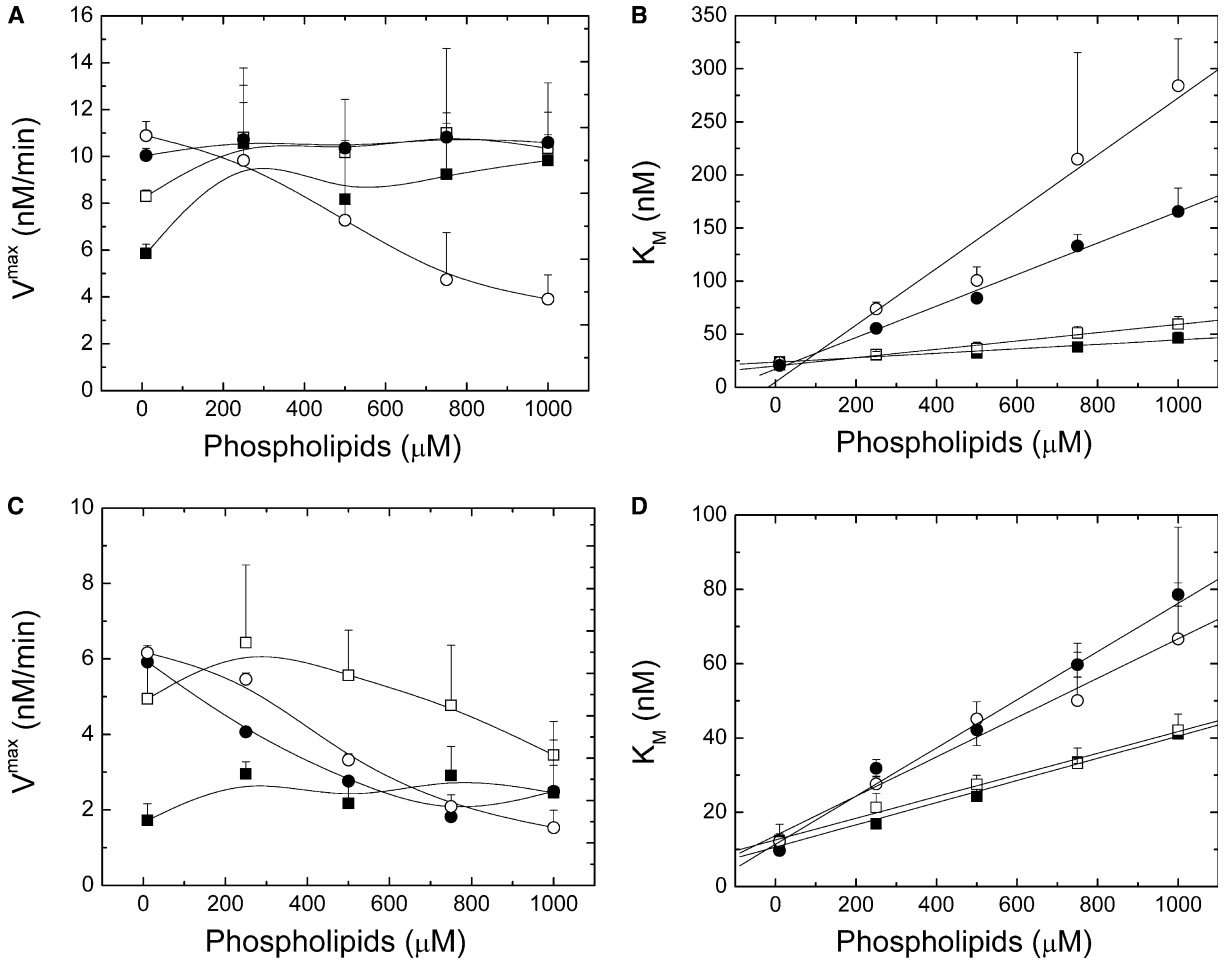

Fig. 6. Effect of the fX and phospholipid concentrations and PtdSer content in phospholipid vesicles on activation of fX. Kinetic parameters for fX activation by fIXa (30 pM) in the presence of fVIIIa and phospholipid vesicles are shown. Mean values (± SE) are presented for two experiments. PtdSer content in the vesicles was 12.5% (■), 25% (□), 37.5% (●), 50% (○). (A) Maximal rate, 12 nM of fVIIIa. (B) Michaelis constant, 12 nM of fVIIIa. (C) Maximal rate, 1.5 nM of fVIIIa. (D) Michaelis constant, 1.5 nM of fVIIIa. Solid lines were drawn by B-spline interpolation for maximal rates and by linear least squares fit for Michaelis–Menten constants.

(K_M at infinitely low [PtdChoPtdSer]) is the real K_M for fX, as no excess phospholipid is present to bind fX and to reduce the free fX concentration. Therefore, intrinsic K_M should be the same for all lines. In the bound substrate model, intrinsic K_M equals the [fX^{free}] concentration required to obtain the fX density on the membrane, at which half of membrane-bound fX is involved in the reaction; therefore, intrinsic K_M is expected to increase with the decrease in PtdSer content. Summarizing, the free substrate model should give a set of lines with different slopes (determined by PtdSer content) and identical intrinsic K_M in the K_M vs. phospholipid concentration plot, whereas the bound substrate model is expected to yield a set of parallel lines.

The results of the experiment at 12 nM of fVIIIa indicated that the reaction of fX activation by intrinsic tenase is likely to follow the free substrate model (Fig. 6A,B). The lines had similar intrinsic K_M values (~20 nM) and the slopes of the lines at 12.5 and 50% PtdSer differed 13-fold, in agreement with the estimations on the basis of q and K_d^X reported for fX–phospholipid interaction [11,12]. At 1.5 nM fVIIIa (Fig. 6C,D), there was little difference in either intrinsic K_M values (~10–12 nM) or the slopes (1.7-fold). This does not correspond exactly to any of the models and most likely reflects a mixed model of fX delivery, e.g. at low phospholipid concentration, fVIIIa could occupy all binding sites on phospholipid vesicles, making the free-substrate mechanism the only possible one, whereas at high phospholipid concentrations, fX may bind mostly to phospholipids and not directly to fVIIIa.

Discussion

This study was aimed at elucidating the mechanism of the fX-activating complex assembly on phospholipid membranes in the course of activation of fX by intrinsic tenase. Specifically, two problems were addressed. The first is the order of assembly of the fX-activating complex. As discussed by Boscovic *et al.* [30], there may be seven possible pathways for assembly of a ternary complex, depending on the intermediate binary complexes formed. In the course of assembly of intrinsic tenase, fX can bind to the preassembled fIXa–fVIIIa complex, or fVIIIa can bind fX and deliver it to fIXa, etc. Formation of the fIXa–fVIIIa complex has been studied extensively in both kinetic and binding experiments [5,15,16] and the role of cofactor fVIIIa has been established in modulating the active site of enzyme fIXa and increasing the number of the bound enzyme molecules. The interaction of fIXa and fX has been studied in fX activation experiments in the absence of fVIIIa [1,31,32]. The interaction of fVIIIa with fX has been studied in a solid phase binding assay [17,18,21] but not in solution or on phospholipid membranes.

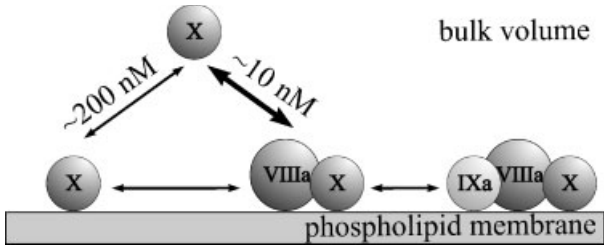

Fig. 7. Possible pathways of *the* fX delivery to *the* fX-activating complex. FX from solution can either directly bind to lipid-bound fVIIIa (free substrate model) or bind the membrane first, followed by *the* formation of the fVIIIa–fX complex (bound substrate model). Subsequently, fVIIIa delivers the substrate to the enzyme in the fX-activating complex.

Another problem is the role of phospholipid membrane in the delivery of fX to the fX-activating complex. There are two principal mechanisms of substrate delivery in a membrane-dependent reaction: the substrate can either bind directly from solution to the enzyme (free substrate model) or bind to the membrane first and subsequently interact with the enzyme by means of two-dimensional diffusion (bound substrate model), as illustrated in Fig. 7. Previous studies disagree with respect to the mechanisms of substrate delivery in the homologous complexes of intrinsic tenase and prothrombinase. That the bound substrate model explains the apparent increase of the Michaelis–Menten constant with the increase of phospholipid concentration suggested that this model works for both phospholipid-dependent reactions [1,33,34]. However, in other studies the rates of prothrombinase [25,35] and intrinsic tenase [31] appeared to be independent of the substrate surface density on phospholipids, consistent with the free substrate model. The existing mathematical models for both reactions [19,34,36–38] are based on the bound substrate model. For the activation of fX by fIXa in the absence of fVIIIa, the bound substrate model was established experimentally [31,39].

In this study, we systematically analyzed the equilibrium binding of all components of the intrinsic fX-activating complex in various combinations to synthetic phospholipid vesicles by flow cytometry in order to detect and quantitate formation of binary complexes, and subsequently analyzed the effect of formation of these complexes on the rate of fX activation. The binding experiments (Fig. 1) detected formation of all three possible binary complexes, with a predominance of

fIXa–fVIII(a) and fVIII(a)–fX. It should be noted that the true binding affinities of individual components of intrinsic tenase for the phospholipid membrane differ by orders of magnitude: ~5–10 nM for fVIII [8,10], ~100–200 nM for fX [12], ~1000 nM for fIXa [9,40]. In our experiments, the binding of coagulation factors was not significantly affected by the presence of factors with a lower affinity used at concentrations below their K_d (i.e. the fVIII binding did not change in the presence of either fIXa or fX, and the fX binding in the presence of fIXa). In contrast, in the presence of factors with a higher affinity, the binding curves changed their form and did not follow the one-site binding equation (e.g. the fIXa and fX binding curves in the presence of fVIII or fVIIIa). This suggests that these factors function as anchors for factors with a lower affinity, providing new high-affinity (10–20 nM) binding sites on the phospholipid surface (fVIII for fIXa or fX, fX for fIXa).

This conclusion was further confirmed in the parallel titration binding experiments, which studied the binding of low-affinity factors as a function of the high-affinity factor binding (Fig. 2). The slopes of the upper curves in panels A, B, and D in their initial parts were close to 1 indicating a 1 : 1 stoichiometry for fIXa–EGR–fVIII(a) and fX–fVIII(a) complexes. In this part of the curves, the concentration of low-affinity factor exceeds the K_d of the binary complex formation, and all molecules of high-affinity factor are in the complex. Previously, two fundamental functions have been ascribed to cofactor fVIIIa in the activation of fX: enhancement of the catalytic constant of the reaction and increase of the amount of phospholipid-bound enzyme fIXa [32]. Based on the obtained data, we hypothesize that, in addition to these functions, fVIIIa is also involved in increasing the amount of phospholipid-bound substrate fX. Interestingly, this anchoring effect did not depend on fVIII activation (Figs 1 and 2), in agreement with a previous study reporting the equally efficient binding of fX to both fVIII and fVIIIa [17].

We next demonstrated that formation of the fVIIIa–fX complex is significant for the functioning of the intrinsic tenase complex. By titrating both fVIIIa and fX (Fig. 4A,B), we revealed a positive correlation between the rate of fXa formation and the fX binding to fVIIIa that suggested a regulatory role of the fVIIIa–fX complex in the activation of fX. This conclusion was confirmed by the finding that the apparent K_M of fX activation is dependent on fVIIIa concentration (Fig. 4C). The obtained function was linear, with a slope of 1.00 ± 0.12 (suggesting a 1 : 1 stoichiometry) and intrinsic K_M of 8.0 ± 1.5 nM that is in agreement with the apparent affinity of the fVIIIa–fX complex (Table 1). These results fit with the hypothesis that the rate of fX activation is regulated by formation of the fVIIIa–fX complex which, in fact, is the true substrate in the fX activation. Other explanations seem less probable: for example, occupation of phospholipids-binding sites with fVIIIa could lead to an increase of apparent K_M [25], but this should be accompanied by a decrease in V_{max} which was not the case in our experiment (see inset in Fig. 4C). Interestingly, K_M dependence on fVIIIa concentration has been observed previously [1] but no explanation for the effect has been proposed. The phospholipid concentration, which provides the half-maximal rate of fXa generation, was also a linear function of fVIIIa concentration (Fig. 5D). This is another argument in favor of the regulatory role of the fVIIIa–fX complex in the activation of fX.

This role of the fVIIIa–fX complex outlines the directions for a further refinement of the model of the intrinsic tenase assembly. First, it should be specified whether fIXa binds directly to the preassembled fVIIIa–fX complex or whether the fX-activating complex is assembled via a quaternary interaction between the fIXa–fVIIIa and fVIIIa–fX complexes. Second, the relative quantitative contribution of the direct fX delivery to the preassembled fIXa–fVIIIa complex and the fVIII-mediated delivery of fX should be assessed, and, evidently, the effect of fIXa and fVIIIa concentrations should be considered.

The most plausible mechanism of the regulation of fX activation by the fVIIIa–fX complex is delivery of the substrate (fX) to the membrane. The rate of fX–phospholipid association was higher in the presence of fVIII (K_d = 32 ± 14 nM) than in its absence (K_d = 118 ± 3 nM) suggesting that the direct binding of fX to membrane-bound fVIII is at least as kinetically favorable as the indirect pathway (Fig. 3). Otherwise, a decrease of the rate should be expected in the presence of fVIII due to a decrease of the number of free binding sites. We performed parallel titrations of fX, phospholipid concentration, and PtdSer content in vesicles (Fig. 6) to elucidate whether the reaction rate is determined by the concentration of free or membrane-bound substrate. As our previous experiments suggested that formation of the fVIIIa–fX complex is a regulating step in the reaction, this was done at two fVIIIa concentrations. Analysis of K_M values revealed that, at high fVIIIa concentrations, the reaction is likely to follow the free substrate model, i.e. fX preferably binds to membrane-bound fVIIIa directly from solution. At low fVIIIa concentrations, there seems to be a mixed case.

An important issue to be discussed in connection with this experiment is the possible segregation of the enzyme, the cofactor, or the substrate to different vesicles due to high phospholipid concentrations. Indeed, quantitation of the vesicles by flow cytometry (data not shown) suggests that at 1000 μM of phospholipids, the molar concentration of phospholipid vesicles exceeds concentration of fIXa molecules by at least an order of magnitude. However, taking into consideration the extremely high dissociation constant of fIXa/phospholipid binding (≫1000 nM), a four orders of magnitude lower dissociation constant for fIXa binding to the membrane-bound fVIII [14], and the low fIXa concentrations used in these experiments (30 pM), it is most likely that phospholipid-bound fIXa will be present only in the form of fIXa–fVIIIa complex. Thus, the enzyme and the cofactor will be present on the same vesicle. Furthermore, the purpose of increasing phospholipid concentration was to regulate the membrane density and volume concentration of the substrate, and the derivation of Eqn (1) does not require all (or even most) vesicles to contain enzyme molecules [25]. Thus, the binding of some substrate molecules to vesicles not containing the enzyme-cofactor complexes does not affect conclusions of this experiment.

Our findings offer an explanation for the existing disagreement on the mechanisms of substrate delivery. First, the binding of fX to the membrane-bound fVIIIa, in addition to its binding to the preassembled fIXa–fVIIIa complex, should be considered. Second, the mechanism of fX delivery to the membrane seems to depend on the conditions of the study, in particular, on fVIIIa concentration.

Our study was performed on synthetic PtdSer/PtdCho (25/75) vesicles as the most well-characterized experimental model, and the physiological relevance of our conclusions requires further verification using activated platelets and other physiological procoagulant surfaces. However, there are indications that the results of this study can be extrapolated to the physiological conditions. For example, parameters of fVIIIa–fX interaction on phospholipid membranes, which we determined (Table 1), are close to those obtained in the study on the coordinate binding of these proteins (K_d ~30 nM) to activated platelets [41].

In conclusion, the experimental evidence of the present study shows that: (a) the high-affinity fVIIIa–fX complex is effectively formed on phospholipid membranes in the course of assembly of the fX-activating complex; and (b) formation of the fVIIIa–fX complex regulates the rate of fX activation, at least under conditions when fVIIIa is in excess over fIXa. Noteworthy, thrombin generation experiments in reconstituted system demonstrated that maximal rates are achieved when < 1% of fIX is activated [42], suggesting that excessive presence of fVIIIa over fIXa may occur under physiological conditions.

Experimental procedures

Reagents

The chromogenic fXa-sensitive substrate *N*-α-((benzyloxy)carbonyl)-D-Arg-Gly-Arg-*p*-nitroanalide dihydrochloride (S-2765) was purchased from Diapharma (West Chester, OH). Bovine serum albumin (BSA), phenylalanine–proline–arginine chloromethyl ketone (PPACK) and human α-thrombin were from Sigma (St. Louis, MO). Bovine brain PtdSer and phosphatidylcholine (PtdCho) from egg yolk were from Avanti Polar Lipids (Alabaster, AL). All other reagents were of analytical quality.

Proteins

Human plasma-derived fVIII was purified from therapeutic fVIII concentrate (Antihemophilic Factor, human, American Red Cross, Rockville, MD) as described previously [26]. Human fIXa and active site-inhibited fIXa–EGR were from Haematologic Technologies (Essex Junction, VT). Human fX and fXa were from Enzyme Research Laboratories (South Bend, IN). For the binding studies, the proteins were labeled with fluorescein as described previously [27]. All proteins were stored at −80 °C in 5–10 μL aliquots and thawed immediately before use. Adequacy of labeled factors was tested in control binding experiments with factors labeled at dye/protein ratios in the range of 0.4–4, which gave identical results.

Preparation of phospholipid vesicles

Vesicles were prepared according to a protocol described previously [28] by extrusion through either 0.1 or 0.8 μm pore size polycarbonate membranes using a mini-extruder device (Avanti Polar Lipids). For binding studies, a lipophilic fluorescent dye 1,1′-dihexadecyl-3,3,3′,3′-tetramethylindocarbocyanine perchlorate [DiIC16(3); Molecular Probes] in ethanol was added at 0.2 mol%. The vesicles were stored at +4 °C and were used within four days of preparation. For binding experiments and for fX activation experiments, 0.8 and 0.1 μm vesicles were used, respectively, unless specified otherwise. Control experiments have shown that kinetic constants of fX activation by intrinsic tenase are similar for these two types of vesicles under conditions of this study.

Binding experiments

Binding of labeled factors to phospholipid vesicles was performed according to the method of Gilbert *et al.* [29] with

minor modifications. Briefly, the proteins were incubated with 0.8 μm phospholipid vesicles in 150 mM NaCl, 2.7 mM KCl, 1 mM $MgCl_2$, 0.4 mM NaH_2PO_4, 20 mM Hepes, 5 mM glucose, 0.5% BSA, pH 7.4 (buffer A) in the presence of $CaCl_2$ (2.5 mM) at 37 °C for 15 min unless specified otherwise. Calcium was always added to buffer A immediately before experiments. Control experiments confirmed that this period was sufficient to achieve equilibrium. When the fVIIIa binding was studied, fVIII was activated by thrombin (1 nM) for 1 min prior to incubation with vesicles, and thrombin was inhibited by PPACK at 1 μM. Samples were diluted 10-fold with buffer A containing 2.5 mM $CaCl_2$, and immediately acquired for 10 s in a FACSCalibur flow cytometer (Becton Dickinson, San Jose, CA). Vesicles were identified by DiIC16(3) fluorescence measured in a FL2 channel. Bound coagulation factor was determined by measuring mean fluorescence intensity of FL2-positive events in a FL1 channel. The fluorescence intensity was converted to the mean number of molecules per vesicle using a calibration curve prepared with a Quantum Fluorescent Microbead Standard for fluorescein (Sigma). Control experiments confirmed that, during the time of sample dilution and analysis, < 5% of the protein dissociated from the vesicles.

fXa generation experiments

Assays were performed in 96-well flat bottom polystyrene plates (Falcon®, Becton Dickinson, Franklin Lakes, NJ). Varying ratios of phospholipid, fIXa, and fVIII were incubated in buffer A in the presence of 2.5 mM $CaCl_2$ at 37 °C. After activation of fVIII by thrombin (final concentration 1 nM) for 1 min, the reaction was initiated by addition of fX. The reaction was stopped after 2 min by addition of ice-cold EDTA to a final concentration of 10 mM. The linearity of fXa production during the first 3 min under various conditions was confirmed in separate experiments (data not shown). Generated fXa was determined from the rate of conversion of a chromogenic substrate S-2765 (final concentration 0.3 mM). The rate of substrate hydrolysis was monitored by absorbance at 405 nm using a Tecan GENios Pro microplate reader (Tecan U.S., Durham, NC) in a kinetic mode and was converted to fXa concentration using a calibration curve prepared with a fXa standard. Control experiments showed that contribution of thrombin used for fVIII activation to the hydrolysis of S-2765 was negligible (data not shown).

Analysis of experimental data

All experiments were performed in triplicate, unless specified otherwise; representative experiments are shown in the figures. The binding and fX activation parameters were obtained by fitting respective curves from independent experiments to a rectangular hyperbola equation using a nonlinear least squares method implemented in MICROCAL ORIGIN 6.0 (Microcal Software, Inc.). The number of newly formed additional binding sites (e.g. the sites provided for fX by fVIIIa) was calculated by subtracting the binding curve for fX alone from the binding curve for fX in the presence of fVIIIa. This method does not take into account potential competition between fX and fVIIIa for the binding sites. To avoid competition effects, only those portions of the binding curves, where the subtracted fX binding did not exceed the obtained specific binding (Fig. 1B inset), were used. For all fits in this study, the R2 value was above 0.98; for the vast majority of experiments, it was above 0.995.

Acknowledgements

We express our appreciation to Drs Gary Moroff and Mikhail V. Ovanesov (American Red Cross) for helpful discussions and careful reading of the manuscript. We are deeply grateful to James Kurtz and Shalini Seetharaman (American Red Cross) for their expert counsel and assistance with flow cytometry technique. This work was supported by grants HL66101 and HL 72929 from the National Institutes of Health awarded to E.L.S., by grant from the Russian Foundation for Basic Research no. 03-04-48338 to F.I.A., and by NATO Collaborative Linkage Grant no. 979210 to E.L.S and F.I.A.

References

1 van Dieijen G, Tans G, Rosing J & Hemker HC (1981) The role of phospholipid and factor VIIIa in the activation of bovine factor X. *J Biol Chem* **256**, 3433–3442.
2 Fay PJ (2004) Activation of factor VIII and mechanisms of cofactor action. *Blood Rev* **18**, 1–15.
3 Venkateswarlu D, Perera L, Darden T & Pedersen LG (2002) Structure and dynamics of zymogen human blood coagulation factor X. *Biophys J* **82**, 1190–1206.
4 Fay PJ, Haidaris PJ & Smudzin TM (1991) Human factor VIIIa subunit structure. Reconstruction of factor VIIIa from the isolated A1/A3–C1–C2 dimer and A2 subunit. *J Biol Chem* **266**, 8957–8962.
5 Gilbert GE & Arena AA (1996) Activation of the factor VIIIa–factor IXa enzyme complex of blood coagulation by membranes containing phosphatidyl-L-serine. *J Biol Chem* **271**, 11120–11125.
6 Erb EM, Stenflo J & Drakenberg T (2002) Interaction of bovine coagulation factor X and its glutamic-acid-containing fragments with phospholipid membranes. A surface plasmon resonance study. *Eur J Biochem* **269**, 3041–3046.
7 Krishnaswamy S, Jones KC & Mann KG (1988) Prothrombinase complex assembly. Kinetic mechanism of

enzyme assembly on phospholipid vesicles. *J Biol Chem* **263**, 3823–3834.
8 Saenko EL, Scandella D, Yakhyaev AV & Greco NJ (1998) Activation of factor VIII by thrombin increases its affinity for binding to synthetic phospholipid membranes and activated platelets. *J Biol Chem* **273**, 27918–27926.
9 Beals JM & Castellino FJ (1986) The interaction of bovine factor IX, its activation intermediate, factor IX alpha, and its activation products, factor IXa alpha and factor IXa beta, with acidic phospholipid vesicles of various compositions. *Biochem J* **236**, 861–869.
10 Gilbert GE, Furie BC & Furie B (1990) Binding of human factor VIII to phospholipid vesicles. *J Biol Chem* **265**, 815–822.
11 Nelsestuen GL & Broderius M (1977) Interaction of prothrombin and blood-clotting factor X with membranes of varying composition. *Biochemistry* **16**, 4172–4177.
12 Cutsforth GA, Whitaker RN, Hermans J & Lentz BR (1989) A new model to describe extrinsic protein binding to phospholipid membranes of varying composition: application to human coagulation proteins. *Biochemistry* **28**, 7453–7461.
13 Gilbert GE, Drinkwater D, Barter S & Clouse SB (1992) Specificity of phosphatidylserine-containing membrane binding sites for factor VIII. Studies with model membranes supported by glass microspheres (lipospheres). *J Biol Chem* **267**, 15861–15868.
14 Mathur A, Zhong D, Sabharwal AK, Smith KJ & Bajaj SP (1997) Interaction of factor IXa with factor VIIIa. Effects of protease domain Ca^{2+} binding site, proteolysis in the autolysis loop, phospholipid, and factor X. *J Biol Chem* **272**, 23418–23426.
15 Duffy EJ, Parker ET, Mutucumarana VP, Johnson AE & Lollar P (1992) Binding of factor VIIIa and factor VIII to factor IXa on phospholipid vesicles. *J Biol Chem* **267**, 17006–17011.
16 Fay PJ, Koshibu K & Mastri M (1999) The A1 and A2 subunits of factor VIIIa synergistically stimulate factor IXa catalytic activity. *J Biol Chem* **274**, 15401–15406.
17 Lapan KA & Fay PJ (1997) Localization of a factor X interactive site in the A1 subunit of factor VIIIa. *J Biol Chem* **272**, 2082–2088.
18 Lapan KA & Fay PJ (1998) Interaction of the A1 subunit of factor VIIIa and the serine protease domain of factor X identified by zero-length cross-linking. *Thromb Haemost* **80**, 418–422.
19 Panteleev MA, Saenko EL, Ananyeva NM & Ataullakhanov FI (2004) Kinetics of factor X activation by the membrane-bound complex of factor IXa and factor VIIIa. *Biochem J* **381**, 779–794.
20 Ahmad SS, London FS & Walsh PN (2003) The assembly of the factor X-activating complex on activated human platelets. *J Thromb Haemost* **1**, 48–59.
21 Nogami K, Freas J, Manithody C, Wakabayashi H, Rezaie AR & Fay PJ (2004) Mechanisms of interactions of factor X and factor Xa with the acidic region in factor VIII, A1 domain. *J Biol Chem* **279**, 33104–33113.
22 McGee MP, Li LC & Xiong H (1992) Diffusion control in blood coagulation. Activation of factor X by factors IXa/VIIIa assembled on human monocyte membranes. *J Biol Chem* **267**, 24333–24339.
23 Giesen PL, Willems GM, Hemker HC & Hermens WT (1991) Membrane-mediated assembly of the prothrombinase complex. *J Biol Chem* **266**, 18720–18725.
24 Butenas S, Branda RF, van't Veer C, Cawthern KM & Mann KG (2001) Platelets and phospholipids in tissue factor-initiated thrombin generation. *Thromb Haemost* **86**, 660–667.
25 van Rijn JL, Govers-Riemslag JW, Zwaal RF & Rosing J (1984) Kinetic studies of prothrombin activation: effect of factor Va and phospholipids on the formation of the enzyme–substrate complex. *Biochemistry* **23**, 4557–4564.
26 Saenko EL, Shima M, Gilbert GE & Scandella D (1996) Slowed release of thrombin-cleaved factor VIII from von Willebrand factor by a monoclonal and a human antibody is a novel mechanism for factor VIII inhibition. *J Biol Chem* **271**, 27424–27431.
27 Kulin S, Kishore R, Hubbard JB & Helmerson K (2002) Real-time measurement of spontaneous antigen–antibody dissociation. *Biophys J* **83**, 1965–1973.
28 MacDonald RC, Macdonald RI, Menco BP, Takeshita K, Subbarao NK & Hu LR (1991) Small-volume extrusion apparatus for preparation of large, unilamellar vesicles. *Biochim Biophys Acta* **1061**, 297–303.
29 Gilbert GE, Sims PJ, Wiedmer T, Furie B, Furie BC & Shattil SJ (1991) Platelet-derived microparticles express high affinity receptors for factor VIII. *J Biol Chem* **266**, 17261–17268.
30 Boskovic DS, Giles AR & Nesheim ME (1990) Studies of the role of factor Va in the factor Xa-catalyzed activation of prothrombin, fragment 1.2-prethrombin-2, and dansyl-L-glutamyl-glycyl-L-arginine-meizothrombin in the absence of phospholipid. *J Biol Chem* **265**, 10497–10505.
31 Beals JM, Chibber BA & Castellino FJ (1989) The kinetic assembly of the intrinsic bovine factor X activation system. *Arch Biochem Biophys* **268**, 485–501.
32 van Dieijen G, van Rijn JL, Govers-Riemslag JW, Hemker HC & Rosing J (1985) Assembly of the intrinsic factor X activating complex – interactions between factor IXa, factor VIIIa and phospholipid. *Thromb Haemost* **53**, 396–400.
33 Rosing J, Tans G, Govers-Riemslag JW, Zwaal RF & Hemker HC (1980) The role of phospholipids and factor Va in the prothrombinase complex. *J Biol Chem* **255**, 274–283.

34 Nesheim ME, Tracy RP & Mann KG (1984) 'Clot-speed', a mathematical simulation of the functional properties of prothrombinase. *J Biol Chem* **259**, 1447–1453.
35 Pusey ML & Nelsestuen GL (1983) The physical significance of K_m in the prothrombinase reaction. *Biochem Biophys Res Commun* **114**, 526–532.
36 Nesheim ME, Tracy RP, Tracy PB, Boskovic DS & Mann KG (1992) Mathematical simulation of prothrombinase. *Methods Enzymol* **215**, 316–328.
37 Bungay SD, Gentry PA & Gentry RD (2003) A mathematical model of lipid-mediated thrombin generation. *Math Med Biol* **20**, 105–129.
38 Kuharsky AL & Fogelson AL (2001) Surface-mediated control of blood coagulation: the role of binding site densities and platelet deposition. *Biophys J* **80**, 1050–1074.
39 Scandura JM & Walsh PN (1996) Factor X bound to the surface of activated human platelets is preferentially activated by platelet-bound factor IXa. *Biochemistry* **35**, 8903–8913.
40 Burri BJ, Edgington TS & Fair DS (1987) Molecular interactions of the intrinsic activation complex of coagulation: binding of native and activated human factors IX and X to defined phospholipid vesicles. *Biochim Biophys Acta* **923**, 176–186.
41 Ahmad SS & Walsh PN (2002) Coordinate binding studies of the substrate (factor X) with the cofactor (factor VIII) in the assembly of the factor X activating complex on the activated platelet surface. *Biochemistry* **41**, 11269–11276.
42 Lawson JH, Kalafatis M, Stram S & Mann KG (1994) A model for the tissue factor pathway to thrombin. I. An empirical study. *J Biol Chem* **269**, 23357–23366.